Regulation of Voltage Dependence of the KAT1 Channel by Intracellular Factors

TOSHINORI HOSHI

From the Department of Physiology and Biophysics, The University of Iowa College of Medicine, Iowa City, Iowa 52242

ABSTRACT The KAT1 channel is a hyperpolarization-activated K^+ channel cloned from the higher plant *Arabidopsis*. The deduced amino acid sequence suggests that its structural organization is similar to that of the *Shaker*-like K^+ channel activated by depolarization. Electrophysiological properties of the KAT1 channel expressed in *Xenopus* oocytes indicate that voltage-dependent activation of the KAT1 channel is not caused by the divalent ion block and that it is intrinsic to the channel. Activity of the KAT1 channel progressively decreases upon patch excision. This rundown of the channel is accompanied by a large shift in the voltage dependence of the channel to a more negative direction. The voltage dependence is also regulated by pH, ATP, and cGMP.

INTRODUCTION

Electrophysiological studies have identified several functionally different classes of voltage-dependent K^+ channels. Delayed-rectifier, A-type, and Ca^{2+}-dependent K^+ channels open in response to depolarization, whereas the inward rectifier channel opens in response to hyperpolarization. Voltage-dependent K^+ channels have been identified not only in animal cells but also in plant cells as well. Both depolarization-activated and hyperpolarization-activated K^+ channels have been characterized in plant cells (Schroeder, 1988; Schroeder, Raschke, and Netur, 1987). These plant K^+ currents have been implicated in stomatal movements in leaves (Schroeder, Hedrich, and Ferandez, 1984; Schroeder et al., 1987).

Anderson, Huprikar, Kochian, Lucas, and Gaber (1992) determined the DNA sequence of a K^+ channel (KAT1) from the higher plant *Arabidopsis* by complementation of yeast mutants deficient in the K^+ uptake. The nucleotide sequence of a very similar protein (AKT1) was also determined by Sentenac, Bonneaud, Minet, Lacroute, Salmon, Gaymard, and Grignon (1992). The deduced amino acid sequences showed that the structural organizations of the KAT1 and AKT1 proteins are similar to those of the depolarization-activated K^+ channels cloned from animal cells in that they probably have six major transmembrane segments (S1 through S6) and that the pore is likely to be formed by the segment between the S5 and S6 segments. Although the KAT1 channel is activated by hyperpolarization, it has a fairly well-defined S4 segment with positively charged residues. The expression in *Xenopus* oocytes showed that KAT1 encodes for a hyperpolarization-activated K^+ channel, resembling some inward-rectifier channels (Schachtman, Schroeder, Lucas, Ander-

J. GEN. PHYSIOL. © The Rockefeller University Press · 0022-1295/95/03/0309/20 $2.00
Volume 105 March 1995 309–328

son, and Gaber, 1992). The KAT1 channel activates slowly in a time-dependent manner in response to a step hyperpolarization (Schachtman et al., 1992; also see Fig. 1). The amino acid sequences of vertebrate K^+ channels activated by hyperpolarization have also been determined; IRK1 (Kubo, Baldwin, Jan, and Jan, 1993), GIRK1 (Kubo et al., 1993*b*), and ROMK1 (Ho, Vassilev, Kanazirska, Lytton, and Herbert, 1993). Unlike the KAT1 and AKT1 channels, these vertebrate inward rectifier channels are thought to contain only two major transmembrane segments in addition to the pore segment. When expressed, the currents from these vertebrate channels increase almost instantaneously upon hyperpolarization (e.g., Kubo et al., 1993*a*).

Further amino acid sequence comparison shows that the KAT1 and AKT1 channels most closely resemble the *Drosophila* eag channel (Warmke, Drysdale, and Ganetzky, 1991), which is a depolarization-activated K^+ channel with noticeable Ca^{2+} permeability (Brüggemann, Pardo, Stühmer, and Pongs, 1993). This eag channel in turn

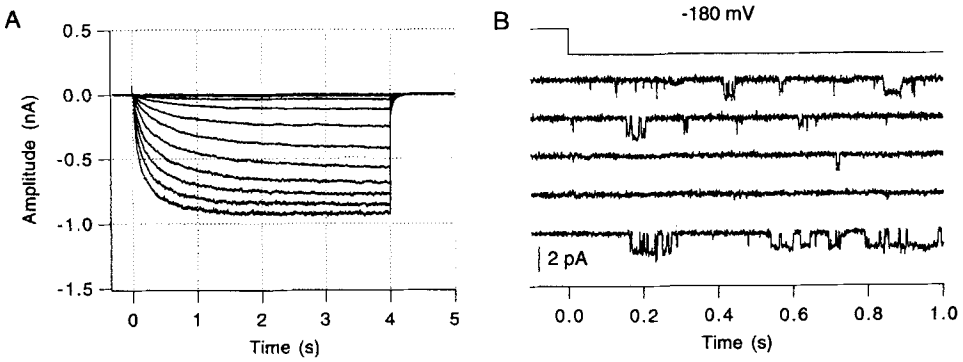

FIGURE 1. Properties of the KAT1 currents. (*A*) Representative KAT1 macroscopic currents recorded in the cell-attached configuration in response to 4-s voltage pulses to −80 to −180 mV in 10-mV increments and then to −50 mV. The data were sampled at 1.25 kHz and filtered at 400 Hz. The pulses were applied every 20 s. (*B*) Representative KAT1 single-channel openings elicited in response to voltage pulses from 0 mV to −180 mV in the inside-out configuration. The data were sampled at 2 kHz and filtered at 500 Hz.

shows a high degree of sequence similarity to the cyclic nucleotide-gated channels (Guy, Durell, Warmke, Drysdale, and Ganetzky, 1991). As in the cyclic nucleotide-gated channels and the eag channel, the KAT1 and AKT1 channels probably contain cyclic nucleotide binding motifs in the carboxyl domains (Anderson et al., 1992; Sentenac et al., 1992). The eag channel has been shown to be modulated by intracellular cAMP (Brüggemann et al., 1993), suggesting that the KAT1 and AKT1 channels may also be modulated by cyclic nucleotides.

Although it is clear that KAT1 codes for a hyperpolarization-activated K^+ channel (Schachtman et al., 1992), detailed information about gating properties of the KAT1 channel is not yet available. The work presented here describes the basic gating properties of the KAT1 channel expressed in *Xenopus* oocytes and how channel gating is regulated. The results are intended to serve as the starting points to

investigate the molecular and biophysical mechanisms involved in the channel gating. The results show that voltage-dependent activation of the KAT1 channel is not caused by internal divalent block. Activation properties of the KAT1 channel are qualitatively more similar to those of the *Shaker* channel than to the previously described vertebrate native inward rectifier channels. The results also show that voltage dependence of the KAT1 channel is regulated by several intracellular factors, including pH, ATP, and cGMP.

MATERIALS AND METHODS

Channel Expression

KAT1 cDNA was provided by the laboratory of R. Gaber, Northwestern University (Evanston, IL). eag cDNA was obtained from the laboratory of G. Robertson, University of Wisconsin (Madison, WI). IRK1 cDNA was obtained from the laboratory of L. Jan, University of California (San Francisco, CA). RNAs were transcribed using T7 polymerase and injected into *Xenopus* oocytes (40 nl per cell) as described previously (Zagotta, Hoshi, and Aldrich, 1989). The recordings were made 2–20 d after injection.

Electrophysiology

The whole-cell KAT1 currents were recorded using a standard two-electrode voltage-clamp amplifier (Warner Instruments, Hamden, CT). The electrodes were filled with 3 M KCl and the input resistance of the current-injection electrode was typically < 1 MΩ. The macropatch and single-channel recordings were obtained using an Axopatch-200A amplifier (Axon Instruments, Foster City, CA). Linear capacitative and leak currents were subtracted using a modified P/n procedure for the macroscopic current data. Most of the macroscopic currents presented were obtained using the macro-patch method. For the single-channel data, the leak and capacitative currents were subtracted using the data sweeps without any openings as the templates. Unless otherwise noted, the holding voltage was 0 mV.

Because the KAT1 current did not decline in amplitude with prolonged hyperpolarization, the macroscopic $I(V)$ curves were often inferred from the KAT1 currents elicited in response to slow voltage ramps. Typically, 10-s voltage ramps from 0 to −180 mV were applied.

Data were acquired and analyzed using a Motorola 68040-based microcomputer equipped with an AD/DA converter (Instrutech, Great Neck, NY). The output of the patch clamp amplifier was low-pass filtered through an eight-pole Bessel filter (Frequency Devices, Haverhill, MA) and digitized at the frequencies indicated. The experiments were carried out at room temperature (20–22°C).

Most of the initial characterizations of the KAT1 currents were based on the data obtained in the cell-attached configuration because the KAT1 currents decreased in amplitude after patch excision. This rundown of the KAT1 channel is described in detail later in the paper. In most of the experiments, multiple cycles of the voltage pulses were given to ensure that the recordings were not severely confounded with the rundown process.

Solutions

The standard "extracellular" solution contained (in millimolar): 140 KCl, 2 $CaCl_2$, and 10 HEPES (*N*-methylglucamine [NMG]), pH 7.2. The "intracellular" solution contained (in millimolar): 140 KCl, 2 $MgCl_2$, 11 EGTA, and 10 HEPES(NMG), pH 7.2. In the cell-attached configuration, the cells were bathed in the intracellular solution. The Mg^{2+}-free, EDTA-internal solution contained (in millimolar): 140 KCl, 11 EDTA, 10 HEPES (NMG), pH 7.2. Assuming

that the deionized water used to make this solution contained 10 μM of Ca^{2+} and Mg^{2+}, the free divalent ion concentration was estimated to be < 10 nM using a public domain program (Chealator® by T.J.M. Schoenmakers). Other solutions used are described in the legends. Test chemicals were added to the standard internal solution and pH readjusted with NMG to 7.2. The junction potentials introduced by the solutions containing these agents were measured to be < 10 mV.

RESULTS

The KAT1 ionic currents activated in a time-dependent manner in response to hyperpolarization (Fig. 1 *A;* Schachtman et al., 1992). The overall activation time course is clearly voltage dependent, getting faster with hyperpolarization. In response to depolarization, no measurable currents were observed. Oocytes injected with water did not show similar ionic currents. The KAT1 currents recorded in the cell-attached configuration did not decline in amplitude with maintained hyperpolarization for at least up to 2 min. This lack of the current decline with maintained hyperpolarization was observed in both the two-electrode voltage-clamp and patch recordings. Many native plant voltage-dependent K^+ currents also appear to lack marked inactivation (e.g., Schroeder, 1988).

A slow, late component in the activation time course was sometimes observed. The relative amplitude of this slow component varied considerably among the oocytes examined, and it was more prominent in the data sweeps recorded at more negative voltages (< −140 mV). Brüggemann et al. (1993) has suggested that a slow activation phase observed in the outward currents recorded from the oocytes injected with eag RNA may be caused by a secondary activation of the endogenous Ca^{2+}-dependent Cl^- current.

The KAT1 channel currents were not noticeably reduced in amplitude by the agents which have been shown to affect the *Shaker* channel with disrupted *N*-type inactivation. Internal tetraethylammonium (TEA) (20 mM), internal and external ShB *N*-type inactivation ball peptide (200 μM) (Zagotta et al., 1990), and external 4 AP (4 mM) failed to affect the KAT1 currents recorded at −160 or −180 mV in any obvious way. It is possible, however, that some of these agents bind to the channel pore but they are "knocked off" very efficiently by the inward K^+ flux. Nifedipine (100 μM), which blocks the *Shaker* channel by interacting with the open state of the channel (unpublished observation), also failed to reduce the KAT1 current. As shown earlier (Schachtman et al., 1992), the KAT1 current was readily blocked by 10 mM external TEA^+. Although external Al^{3+} has been shown to block the hyperpolarization-activated K^+-currents in *Vicia faba* guard cells (Schroeder, 1988), it did not markedly affect the KAT1 currents (400 μM).

Fig. 1 *B* shows representative KAT1 single-channel currents recorded in the outside-out configuration in response to voltage pulses to −180 mV. At this voltage, the single-channel current amplitude was ~1.2 pA when both the intracellular and extracellular solutions contained 140 mM KCl, corresponding to a single-channel conductance of ~5–6 pS (cf., Schachtman et al., 1992). These inward openings can be distinguished from the endogenous channels in the oocyte using several criteria: (*a*) time-dependent and voltage-dependent activation; (*b*) fast deactivation kinetics at positive voltages; and (*c*) disappearance after patch excision, which is described in

detail later. As seen with most other ion channels, the KAT1 channel openings, which had a mean dwell time of ~10 ms, were interrupted by short closures. Although the macroscopic KAT1 currents did not decline with maintained hyperpolarization for at least a few minutes, the KAT1 channel entered a relatively long-lasting closed state with a mean dwell time >50 ms. These fast and slow closed states may be analogous to the Cf and Ci states of the *Shaker* channel as described by Hoshi, Zagotta, and Aldrich (1994).

Origin of the Voltage Dependence

In many inward-rectifier channels, voltage-dependent block by internal Mg^{2+} contributes markedly to the overall voltage dependence (for review, see Matsuda, 1991). Voltage-dependent activation of the KAT1 current could in part come from voltage-dependent block of the channel by internal divalent ions and/or by the channel protein's intrinsic voltage dependence. The origin of the voltage-dependent activation of the KAT1 current was examined by analyzing the open-channel current-voltage $i(V)$ relation and by recording the macroscopic KAT1 currents in the presence of EDTA.

Voltage-dependent block by internal Mg^{2+} often results in the rectification of $i(V)$ such that the outward K^+ flux is preferentially inhibited (e.g., Burton and Hutter, 1990). The KAT1 open channel $i(V)$ curve was obtained in response to voltage ramps. A representative single KAT1 current recorded in response to a voltage ramp is shown in Fig. 2 *A*. Only the single-level "open" segments of the currents elicited were conditionally averaged to obtain the "composite" $i(V)$ curve (Fig. 2 *B*). The KAT1 $i(V)$ curve is roughly linear in the voltage range of −70 to −140 mV, where the open channel probability changes with voltage very steeply (see Fig. 4). Consistent with the single-channel results, the open-channel $i(V)$ curve estimated from the macroscopic "instantaneous" tail currents did not rectify markedly in the same voltage range (Fig. 2 *B*). Thus, the KAT1 open channel $i(V)$ alone does not account for the overall voltage dependence of the KAT1 current.

The KAT1 currents activated in response to hyperpolarization and closed upon depolarization even when the internal divalent ions were chealated with 11 mM EDTA (Fig. 3). The free divalent ion concentration was calculated to be <10 nM in this solution. Furthermore, increasing the internal free Ca^{2+} to 100 μM or addition of 2 mM $MgCl_2$ to the internal solution did not markedly change the voltage dependence of the KAT1 current.

Voltage-dependent Activation

The macroscopic conductance-voltage $G(V)$ curve was obtained from the tail currents (Fig. 4 *A*). The $G(V)$ curve shows that the probability of the channel being open increases noticeably at ~−80 mV and saturates at ~−190 mV. The data shown in Fig. 4 *A* are best fitted with a Boltzmann function raised to the 3.3rd power with $V_{0.5} = -96$ mV and $z = 1.4$. The semilogarithmic plot of the $G(V)$ data also show that the 3.3rd power of the Boltzmann function fits better than a simple Boltzmann function (Fig. 4 *B*), especially at the voltages where the open probability is small. If four identical KAT1 subunits form one functional KAT1 channel as shown for the *Shaker* channel (MacKinnon, 1991) and if these subunits function independently, the G(V)

could be fitted with the fourth power of a Boltzmann function. The $G(V)$ was best fitted with the equivalent charge of 1.3 and the half activation voltage of −91 mV if the fourth power Boltzmann function is assumed. These parameters are intended as the data description parameters only and the mechanistic interpretations are not

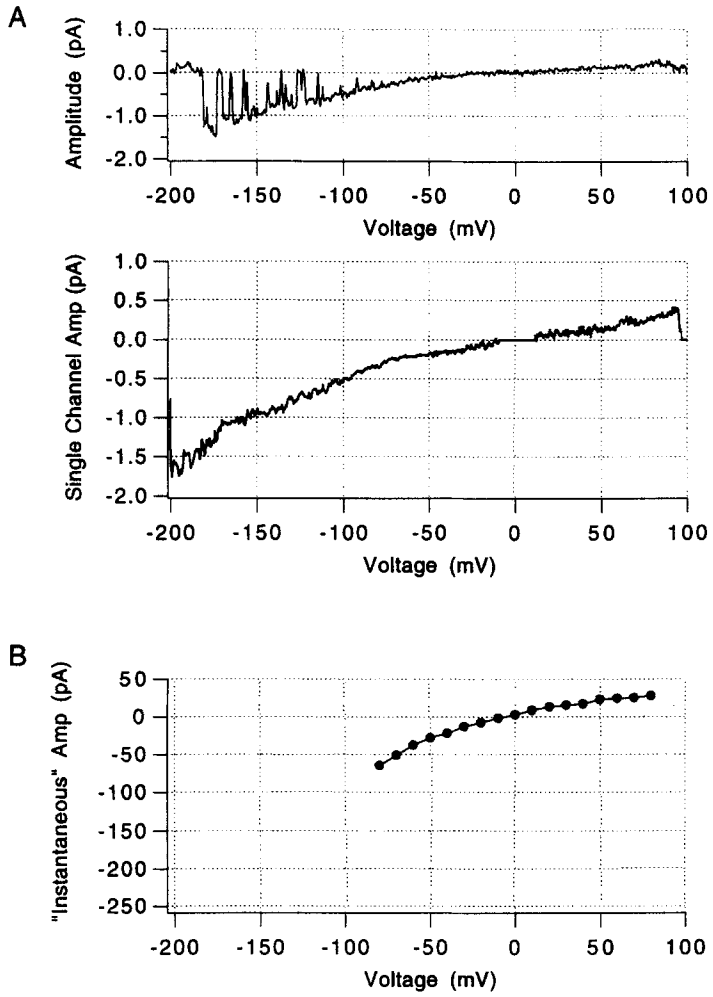

FIGURE 2. Open channel $i(V)$ curve of the KAT1 channel. (*A*) A representative KAT1 channel openings elicited in response to a voltage ramp from −200 to +100 mV (*top*). The composite single KAT1 channel $i(V)$ is shown below. The recordings were made in the outside-out configuration. (*B*) The "instantaneous" tail currents. The KAT1 currents were elicited by 2-s voltage pulses to −180 mV and then depolarized to the test voltages. The tail currents were fitted with single exponentials and the extrapolated time zero currents are plotted.

necessarily implied. The inferred equivalent charge value of five per channel is considerably less than that estimated for the *Shaker* channel, ~12–16 equivalent charges per channel using a variety of methods (Schoppa, McCormack, Tanouye, and Sigworth, 1992; Zagotta et al., 1994*b*). This difference may be attributed to the

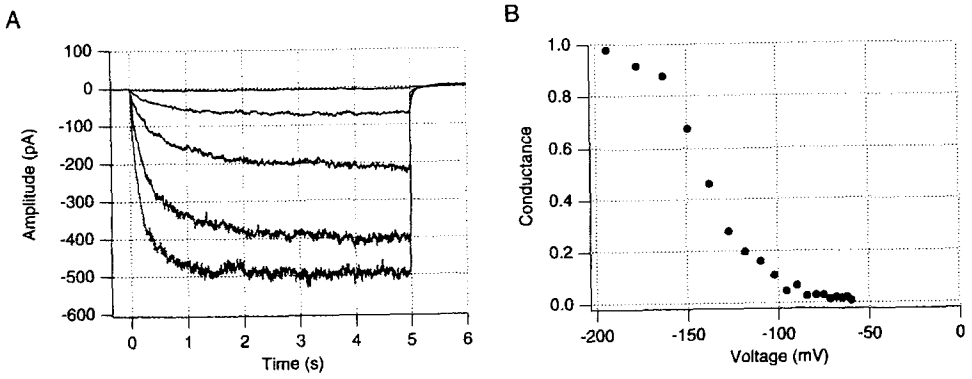

FIGURE 3. (*A*) Representative KAT1 currents recorded in the inside-out configuration with 11 mM EDTA. The currents were recorded in response to 5-s pulses to −80, −127, −150, −177, and −194 mV. (*B*) The KAT1 macroscopic tail $G(V)$ curve in the presence of 11 mM EDTA.

difference in the number of positively charged residues in the respective S4 segments.

By analyzing the voltage dependence of different kinetic parameters, it is possible to infer how many equivalent charges are associated with different conformational

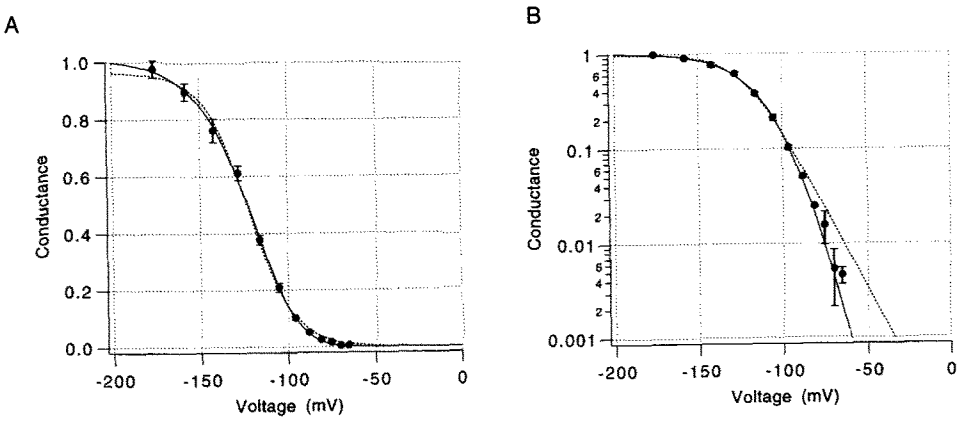

FIGURE 4. (*A*) Macroscopic $G(V)$ curve obtained from the tail current measurements. The tail currents were measured at −100 mV after voltage pulses longer than 5 s. The tail currents were fitted with a single exponential and the time zero current amplitudes were extrapolated. The $G(V)$ was fitted with the following function,

$$G(V) = \left(\frac{1}{1 + e\left(\frac{-(V - V_{0.5})zF}{RT}\right)}\right)^n,$$

where R, T, and F have their usual meanings. $V_{0.5}$ is the voltage where the Boltzmann distribution is equal to 0.5 and z is the equivalent charge. The error bars represent the standard error of the mean. (*B*) A semilogarithmic plot of the KAT1 $G(V)$ curve shown in *B*. In both *A* and *B*, the solid curve was drawn with $V_{0.5} = -96$, $q = 1.4$ and $n = 3.3$ and the dotted curve was drawn with $V_{0.5} = -1.24$, $q = 1.8$, and $n = 1$.

changes of the channel. Voltage dependence of the closing transitions near the open state was estimated by examining the tail currents. Overall, the tail current kinetics was voltage dependent, getting faster at more positive voltages. The KAT1 tail currents recorded at different voltages are shown in Fig. 5. At the voltages where the steady state open probability is negligible, the tail current kinetics was described by a single exponential. Voltage dependence of the time constants is plotted in Fig. 5 *B* and fitted with a single exponential with an equivalent charge of 0.7. At the extreme positive voltages, the tail time constant did not change as much as expected from the simple exponential voltage dependence (see Zagotta, Hoshi, Dittman, and Aldrich, 1994*b*). Using the identical and independent subunit assumption stated above, the tail voltage dependence suggests that ~50% of the total charge movement involved in the overall channel activation is associated with the closing transitions near the open state.

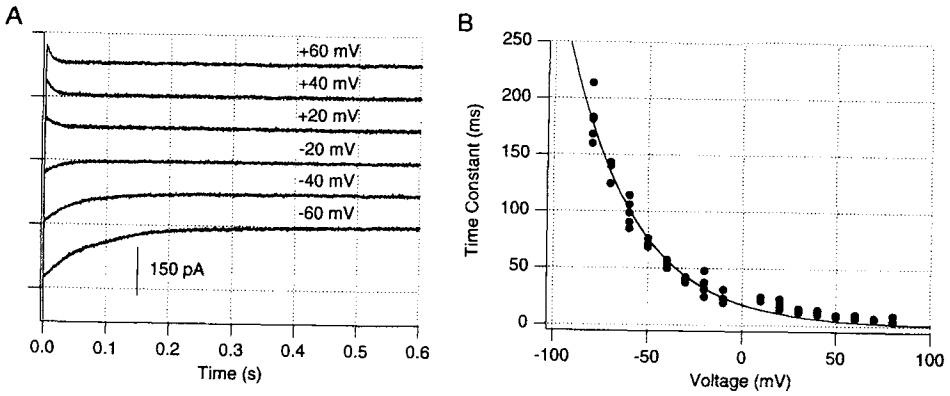

FIGURE 5. Voltage dependence of the tail current kinetics. (*A*) Representative KAT1 tail currents recorded at the voltages indicated after 1-s pulses to −160 mV. Single exponential fits are also shown superimposed. The tail currents were shown offset to facilitate comparison. All the tail currents shown declined to the zero-current level. (*B*) Voltage dependence of the tail time constants. The time constants were fitted with a single exponential with an equivalent charge of 0.7.

G(V) Curves with Different External [K⁺]

In many native inward rectifier channels previously studied (e.g., Cohen, DiFrancesco, Mulrine, and Pennefather, 1989; Pennefather, Oliva, and Mulrine, 1992) and in IRK1 expressed in *Xenopus* oocytes (Kubo et al., 1993), the macroscopic $I(V)$ curves could be shifted along the voltage axis by manipulating the K^+ equilibrium voltage, typically by changing the external $[K^+]$ concentration. Voltage dependence of plant inward-rectifier currents, however, appear to be independent of external $[K^+]$ (Schroeder, 1988). Consistent with this observation, the KAT1 macroscopic $I(V)$ curve obtained using the two-electrode voltage clamp was not markedly affected by reducing the external $[K^+]$ concentration from 140 to 40 mM, which shifts the Nernst voltage for K^+ by ~30 mV to a more negative direction.

Activation Kinetics

Activation kinetics of many native inward rectifier channels with intrinsic voltage dependence follows a simple exponential time course, which is often preceded by an instantaneous current jump (Pennefather et al., 1992; Silver and DeCoursey, 1990). The KAT1 currents activated following a sigmoidal time course, suggesting that the channel transverses several closed states before opening (Fig. 6). This sigmoidal activation time course was not affected by the different leak subtraction procedures used. Sigmoidal properties of the activation process at different voltages can be compared by scaling the data along the time and amplitude axes so that the slopes at the half maximum amplitudes are the same (Zagotta et al., 1994*b*; Fig. 6 *B*). This procedure effectively normalizes the delay involved in the activation relative to the overall activation rate. When the activation time course at different voltages are

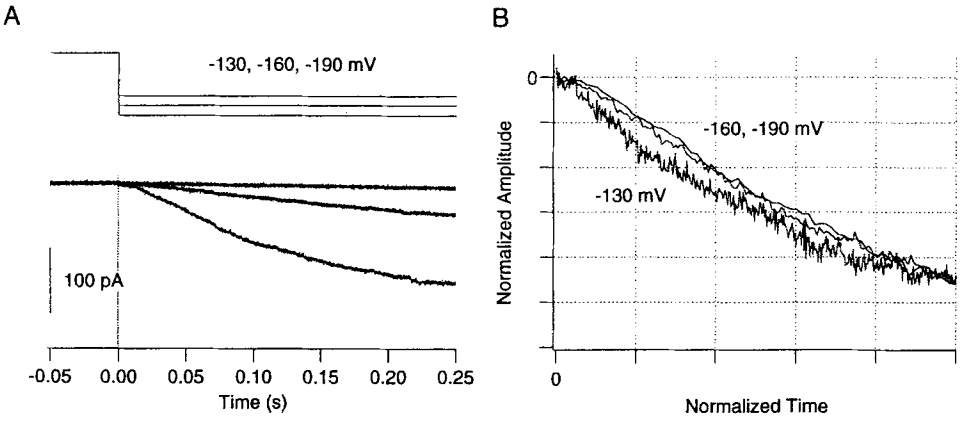

FIGURE 6. Sigmoidal activation of the KAT1 currents. (*A*) The KAT1 currents were recorded in response to voltage pulses to −130, −160, and −190 mV from the holding voltage of 0 mV. The data were filtered at 6 kHz and digitized at 20 kHz. (*B*) The "sigmoidicity" of the KAT1 currents shown in *A*. The currents were scaled both in amplitude and time so that the slopes of the currents at the half maximum levels are the same (Zagotta et al., 1994*b*).

compared in this way, the activation sigmoidicity is not markedly dependent on the voltage (−160 to −190 mV). As found with the *Shaker* channel (Zagotta et al., 1994*b*), the voltage-independent sigmoidicity in this voltage range suggests that the multiple opening transitions in the KAT1 channel may be associated with similar equivalent charges. At −130 mV, however, the activation is less sigmoidal than at −160 or −190 mV. This could be explained if the rate constant for the first closing transition is slow (Zagotta et al., 1994*b*). The sigmoidal activation of the KAT1 current was not affected by the holding voltage (from −50 to +50 mV). This observation limits the number of closed states that the channel has to transverse.

Rundown of the KAT1 Channel

The macropatch and single-channel data presented thus far were mostly obtained in the cell-attached configuration or in the inside-out configuration within the first

several minutes of the patch excision. This was necessary because the KAT1 currents decreased in amplitude after patch excision. Fig. 7 shows the peak KAT1 current amplitudes elicited in response to the voltage pulses to −160 mV. In the cell-attached configuration, the current amplitude was stable. However, after the patch excision (*first arrow*), the current amplitude progressively declined. Time course of this current decline or the rundown process was very variable among the patches examined. In some patches, the rundown was complete within a few minutes as shown. In others,

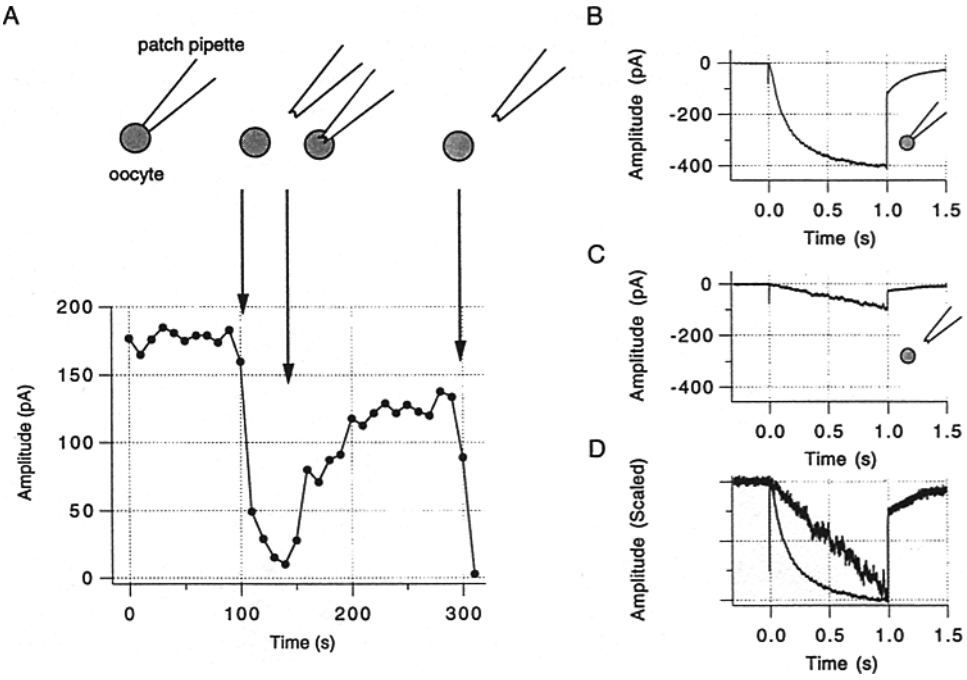

FIGURE 7. Rundown of the KAT1 currents. (*A*) Peak amplitudes of the KAT1 currents elicited in response to 2-s pulses to −160 mV were plotted. At the first arrow, the patch was excised. At the second arrow, the patch was "crammed back" into the oocyte. At the third arrow, the patch was positioned away from the oocyte again. (*B*) The KAT1 current elicited at −160 mV in the cell-attached configuration. (*C*) The KAT1 current at −160 mV in the inside-out configuration. (*D*) The KAT1 currents recorded in the cell-attached and in the inside-out configurations as shown in *B* and *C* are scaled to compare the activation time course.

however, the rundown was much slower and incomplete, and the stable KAT1 currents could be recorded for 5–10 min. The time course and completeness of the KAT1 current rundown appeared to correlate negatively with the amount of "cytoplasmic" material associated with the patches as visually observed: the currents recorded from the "clean" patches without much cytoplasmic material often declined in amplitude rapidly. In addition to the changes in the peak current amplitude, the rundown of the KAT1 current was also accompanied by a marked slowing of the

activation time course. The currents obtained in the cell-attached and the inside-out configurations are scaled and compared in Fig. 7 *D*.

The rundown process affected the KAT1 current amplitude by shifting its voltage dependence. Because it was not practical to obtain the complete macroscopic $G(V)$ curves during the rundown process using step voltage pulses, the macroscopic ramp $I(V)$ curves were used to infer the KAT1 steady state macroscopic $G(V)$ properties. Fig. 8 shows the macroscopic $I(V)$ curves obtained at different times after patch

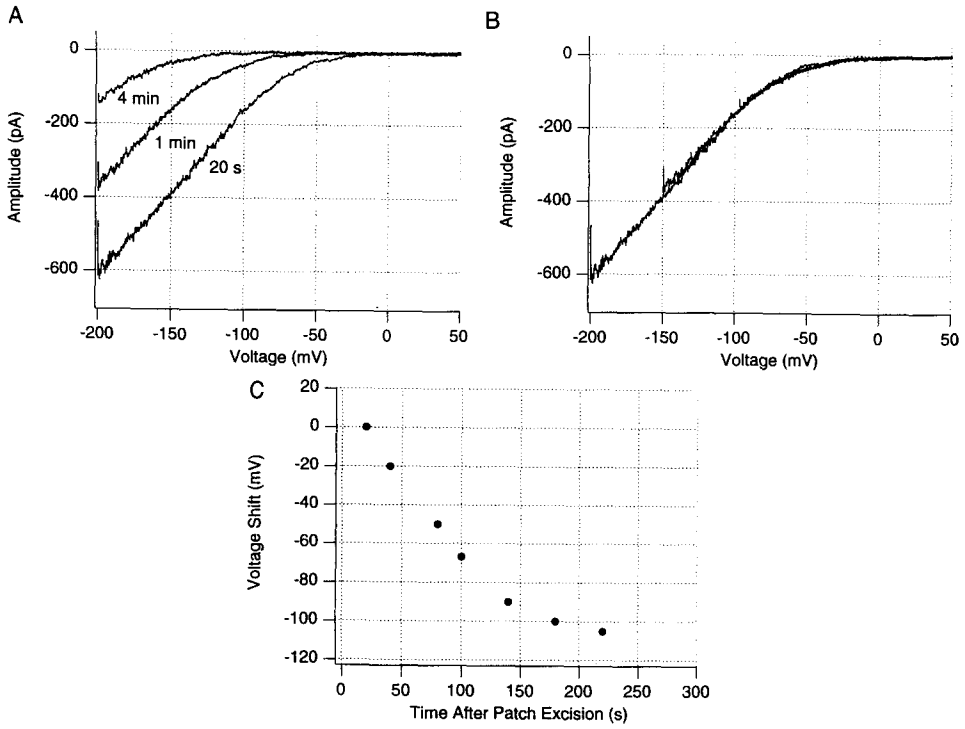

FIGURE 8. The KAT1 ramp $I(V)$ curves during the rundown. (*A*) The ramp $I(V)$ curves recorded at 20 s, 1 and 4 min after the patch excision. The ramp $I(V)$ curves were elicited by 10 s voltage ramps from +50 to −180 mV. (*B*) Ramp $I(V)$ curves obtained 1 and 4 min after the patch excision shown in (A) were shifted along the voltage axis to superimpose on the $I(V)$ curve obtained 20 s after the patch excision by eye. (*C*) The voltage shifts required to superimpose the ramp $I(V)$ curves recorded during the rundown.

excision. The I(V) curves could be superimposed roughly if they were shifted along the voltage axis (Fig. 8 *B*). The voltage offsets required to superimpose the $I(V)$ curves recorded during the rundown process are also shown (Fig. 8 *C*). If the number of functional KAT1 channels decreased during the rundown, the $I(V)$ curves should be superimposed after scaling their amplitudes. This was not generally observed. It is often difficult to determine which factors (*a*) the single-channel $i(V)$, (*b*) the equivalent charge, or (*c*) the rate constant value at 0 mV are responsible for the shift in

macroscopic ramp $I(V)$. The most straight forward explanation is that the rate constant values at 0 mV changed without affecting the equivalent charge.

The results suggest that the KAT1 rundown is a voltage-shift phenomenon involving a shift of > 100 mV. This shift in the voltage dependence accounts for the changes in the kinetics of the KAT1 currents observed during the rundown (see Fig. 7 *D*).

Patch Cramming

The rundown of the KAT1 current was reversed by patch cramming (Kramer, 1990) where the patch was inserted back into the oocyte cytoplasm to expose the patch internal surface to the cytoplasmic factors. Fig. 7 *A* shows that after the KAT1 current had declined to ~10% of that recorded in the cell-attached configuration, patch cramming (Fig. 7 *A*, *second arrow*) restored the current back to 70% of the original value. The patch cramming also restored the kinetics of the KAT1 channel activation. When the patch was positioned away from the oocyte cytoplasm (*third arrow*), the KAT1 current declined again. These results suggest that the KAT1 channel activity is regulated by some intracellular factors, which are lost when the patch is excised. Restoration of the KAT1 channel activity by patch cramming was reliably observed.

ATP Retards the KAT1 Channel Rundown

Rundown of the KAT1 current was often reversed by addition of ATP to the intracellular solution. Fig. 9 *A* shows that the KAT1 current recorded in the inside-out configuration was enhanced by addition of 2 mM ATP. The enhanced KAT1 channel activity was often maintained even when ATP was removed from the intracellular solution (see Fig. 9 *B*). The ATP concentration as low as 0.1 mM was effective in reversing the channel rundown. This effect of ATP was, however, variable among the patches examined, and its efficacy was much more variable than that of the patch cramming method. In some of these experiments where ATP did not markedly restore the channel activity, the subsequent patch cramming did increase the current amplitude, suggesting that ATP may not be the sole factor required for the KAT1 channel to function. Although no quantitative observations were made, the ability of internal ATP to reverse the rundown process may be positively correlated with the amount of cytoplasmic material associated with the macropatches.

The following experimental treatments did not slow the KAT1 channel rundown or restore the KAT1 current after the patch excision: (*a*) different free Ca^{2+} concentrations (10, 100 nM); (*b*) internal cAMP (5 mM); (*c*) internal cGMP (2 mM); (*d*) internal glutathione (5 mM); (*e*) different internal pH (6.2, 7.2, 7.5); (*f*) internal GTP (1 mM); (*g*) Internal GTP-γ-S (1.6 mM).

A nonhydrolyzable analogue of ATP, AMP-PNP, was applied to see if it could restore the KAT1 channel function. Fig. 9 *B* shows that AMP-PNP (1 mM Li salt) failed to restore the KAT1 channel function although the subsequent ATP application was effective (n = 3). LiCl (10 mM) did not obviously affect the rundown or the restoration of the channel activity by ATP. The results suggest that ATP hydrolysis is involved in maintaining the KAT1 channel function. In some experiments, neither AMP-PNP nor ATP was effective in restoring the KAT1 channel activity (n = 2).

At a higher concentration (10 mM), AMP-PNP increased the current amplitude in

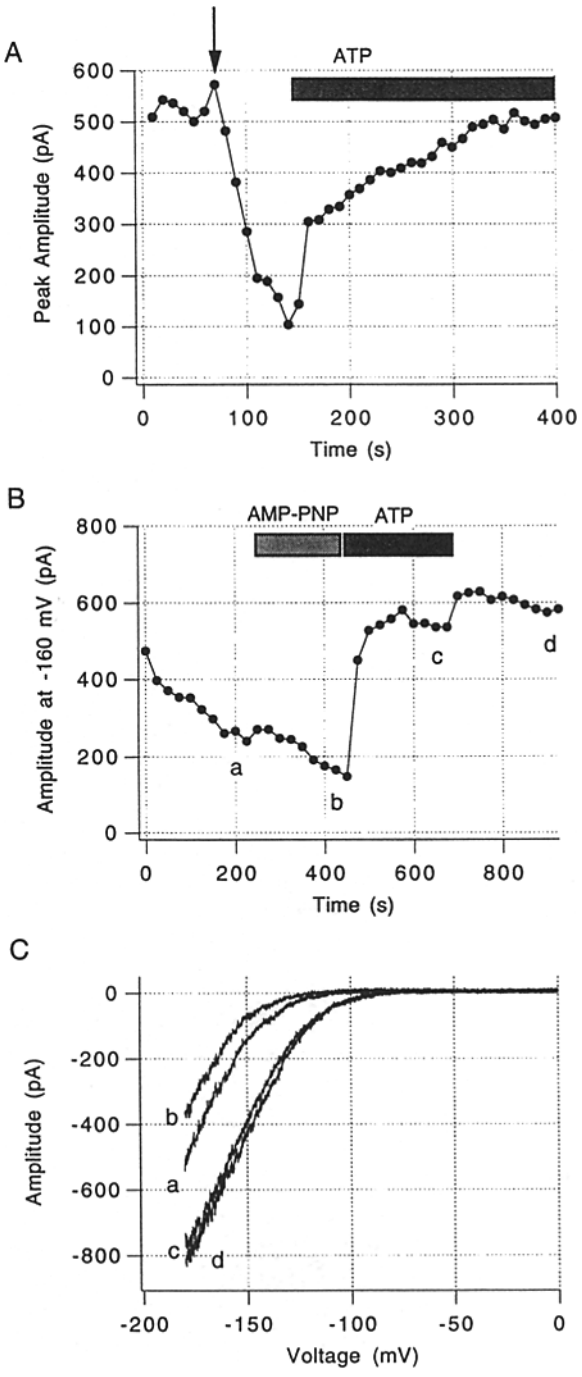

FIGURE 9. (*A*) Internal ATP restores the KAT1 channel activity. Peak KAT1 current amplitudes recorded in response to 1-s voltage pulses at −160 mV from the holding voltage of 0 mV are plotted against the time after the patch excision. At the arrow, the patch was excised. 2 mM ATP (K salt, Sigma Chemical Co.) was applied to the internal surface. (*B*) A nonhydrolyzable analogue of ATP, AMP-PNP, does not restore the KAT1 channel activity. The KAT1 current amplitudes at −160 mV elicited by voltage ramps from +50 to −180 mV are plotted. AMP-PNP, (1 mM Li salt, Sigma Chemical Co.) was perfused and the KAT1 current continued to decline. ATP (1 mM K salt, Sigma Chemical Co.) was then perfused and the KAT1 current amplitude increased. (*C*) Ramp *I*(*V*) curves obtained before, during and after the AMP-PNP and ATP applications.

some experiments but the effects were much less than those of the subsequent 10 mM ATP applications. The effects of ADP, AMP and adenosine hemisulfate were also examined. ADP (1 mM) was generally ineffective in restoring the KAT1 channel activity. However, as in the case of AMP-PNP, at a higher concentration (10 mM), ADP enhanced the KAT1 channel activity in some experiments slightly, although the effects in general were much smaller than those observed with ATP. AMP (K salt, 1 mM), and adenosine hemisulfate (1 mM) were not generally effective in restoring the KAT1 channel activity.

Because the differential effects of ATP and AMP-PNP suggest that ATP hydrolysis may be involved in the KAT1 channel rundown, the effects of protein kinase A (PKA), bacterial alkaline phosphatase (BAP), and calf intestinal phosphatase (CIP) were also examined. PKA catalytic subunit (1 μg/μl, Sigma Chemical Co.; 30 U/μl, Promega Corp.) in the presence of ATP in the standard solution containing 2 mM $MgCl_2$ did

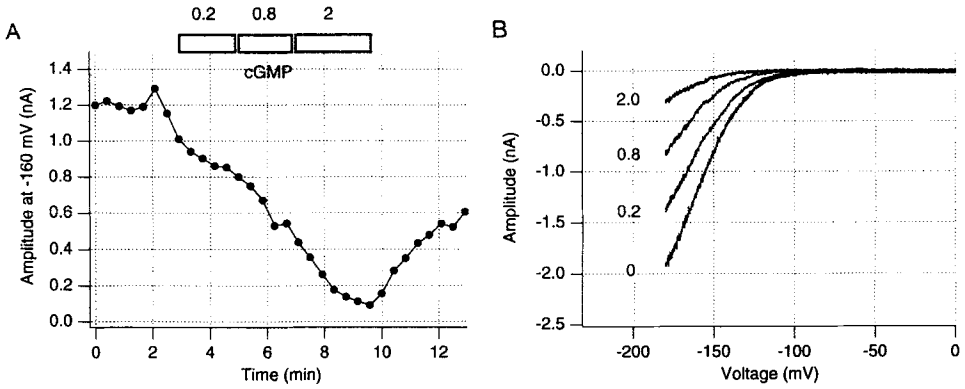

FIGURE 10. The KAT1 channel activity is modulated by cGMP. (*A*) The KAT1 current amplitudes at −160 mV elicited by voltage ramps from 0 to −180 mV are plotted. In this patch, the rundown was very slow and incomplete. 0.2, 0.8, and 2 mM cGMP (Sigma Chemical Co.) were applied. The internal solution did not contain any added ATP. (*B*) The KAT1 ramp $I(V)$ curves in the presence of different cGMP concentrations.

not markedly enhance the KAT1 current (n = 4). BAP (up to 2 U/μl, GIBCO/BRL) and CIP (1 U/μl, NEB) applications for >5 min in the absence of added ATP did not markedly accelerate the KAT1 channel rundown (n = 4 and 1, respectively).

cGMP Modulates the KAT1 Channel Activity

The amino acid sequence analysis indicates that the KAT1 and AKT1 channels contain putative cyclic nucleotide binding domains in the carboxyl segments (Anderson et al., 1992; Sentenac et al., 1992). When cGMP was applied to the intracellular side without any added ATP, the KAT1 ramp $I(V)$ curve shifted to a more negative direction in a concentration dependent manner (Fig. 10). The KAT1 macroscopic $I(V)$ curves recorded at different cGMP concentrations were roughly superimposed by shifting along the voltage axis. Unlike the effect of ATP, which often persisted even after washing with ATP-free solution, this effect of cGMP was consistently

reversible. However, because of the rundown process, it was difficult to perform systematic concentration-dependence studies. When cGMP was applied concurrently with ATP (1 mM), cGMP was much less effective, suggesting that ATP and cGMP have antagonistic effects. cAMP (up to 2 mM) did not have similar effects.

Voltage Dependence Shift by Low pH

The results suggest that the rundown, ATP, and cGMP shift the voltage dependence of activation. Lowering intracellular pH (pH_{in}) can also regulate the voltage dependence of the KAT1 channel. Fig. 11 compares the KAT1 macroscopic currents recorded at pH_{in} = 6.2 and pH_{in} = 7.2, in the presence of ATP to slow down the rundown process. At a given voltage, the activation kinetics at pH_{in} = 6.2 is noticeably faster than that at pH_{in} = 7.2 (Fig. 11 *A*). Furthermore, at pH_{in} = 6.2, the KAT1 macroscopic currents declined in amplitude with time when recorded at the voltages more negative than −160 mV, possibly unmasking a slow inactivation process. The macroscopic $G(V)$ curves obtained from the tail currents at pH_{in} = 6.2 and pH_{in} = 7.2 are compared in Fig. 7 *C*. One of the main effects of lowering pH_{in} from 7.2 to 6.2 is to shift the overall voltage dependence to a more positive direction by ~50 mV without markedly affecting the steepness of the activation curve. Consistent with this idea, the currents recorded at pH_{in} = 6.2 and pH_{in} = 7.2 superimpose well if the voltage-shift of 50 mV is taken into account (Fig. 11 *D*). Lowering internal pH probably affected the single channel $i(V)$ as evidenced by the cross-over of the two $I(V)$ curves as shown in Fig. 11 *C*. A similar cross-over effect was also observed when the $I(V)$ curves were constructed from the currents observed in response to step voltage pulses. If we assume that subunits of the KAT1 channel are identical and independent, the voltage shift can be interpreted in terms of the changes in the values of the rate constants at 0 mV. The observed shift in the $G(V)$ curve of 60 mV by the internal pH change corresponds to a 35-fold change in the equilibrium constant, assuming that each subunit carries an equivalent charge of 1.5 (see Fig. 4).

Although lowering pH_{in} to 6.2 shifts the KAT1 channel activation curve to a more positive direction, opposite of that involved in the rundown process, the rundown was observed even at pH_{in} = 6.2 in the absence of ATP. Changing external pH from 7.2 to 6.2 did not have marked effects on the KAT1 currents.

Comparison of the KAT1 Channel with Other K^+ Channels

The amino acid sequence of the KAT1 channel is closely related to the *Drosophila* eag channel even when the presumed cytoplasmic segments are excluded in the comparison. It has been shown that subunits of certain delayed rectifiers can form heteromultimeric channels when their RNAs were coinjected into *Xenopus* oocytes (e.g., Ruppersberg, Schroter, Sakmann, Stocker, Sewing, and Pongs, 1990) whereas other channel subunits do not appear to form heteromultimeric channels, representing functionally independent groups (Salkoff, Baker, Butler, Covarrubias, Pak, and Wei, 1992). KAT1 and eag RNAs were coinjected to see if they form heteromultimeric channels. If they do, it is expected that voltage dependence of the resulting currents may be altered. The depolarization activated-currents recorded from the cells injected with both eag and KAT1 RNAs were not markedly different from the depolarization-activated currents recorded from the oocytes injected with eag RNA

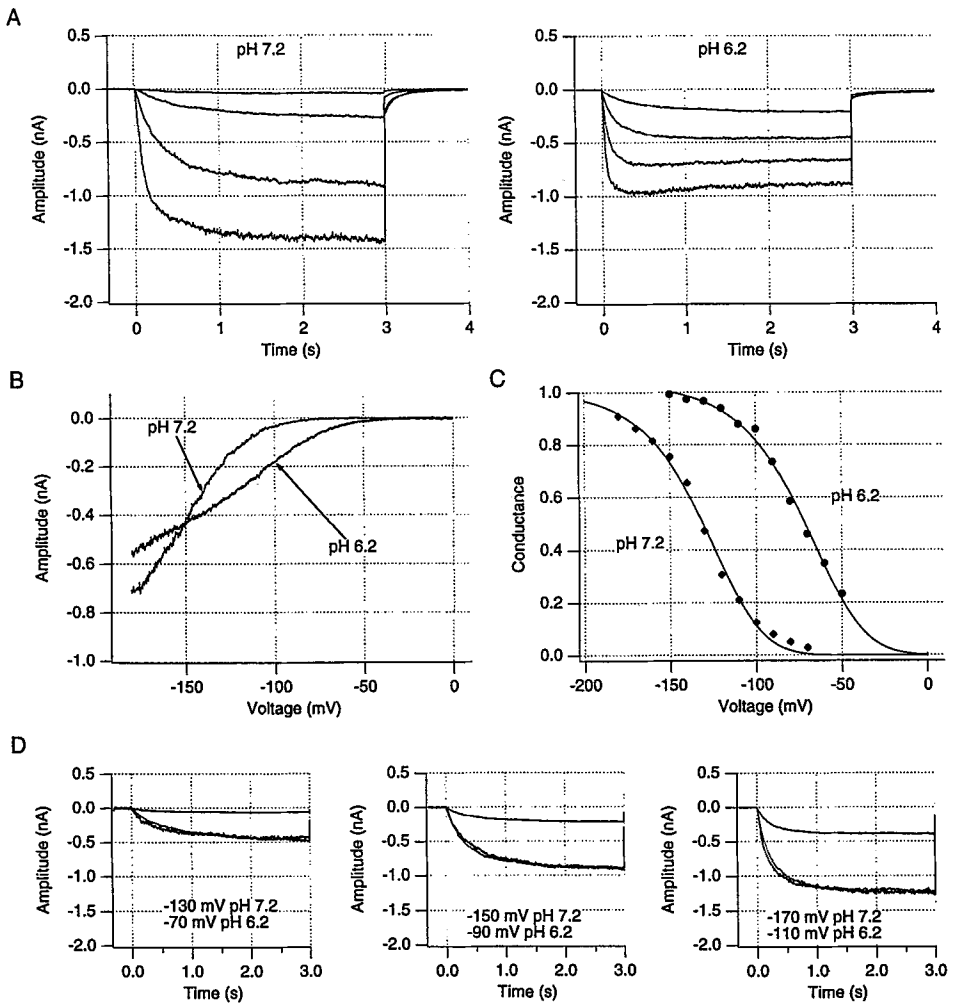

FIGURE 11. Effects of low internal pH on the KAT1 currents. (*A*) The KAT1 currents recorded at pH_{in} = 7.2 (*left*) and pH_{in} = 6.2 (*right*) in the inside-out configuration. The pH 6.2 internal solution contained (in millimolar):140 KCl, 2 $MgCl_2$, 11 EGTA, 10 MES (NMG), pH 6.2. The internal solutions also contained 10 mM ATP (K salt, Sigma Chemical Co.). The records were taken at −90, −120, −150, and −180 mV. (*B*) The KAT1 ramp $I(V)$ curves recorded at pH_{in} = 6.2 and pH_{in} = 7.2 (*C*) The macroscopic tail $G(V)$ curves obtained at pH_{in} = 6.2 and pH_{in} = 7.2. The data at pH_{in} = 7.2 were fitted with $V_{0.5}$ = −93, q = 1.1 and n = 4 and the data at pH_{in} = 6.2 were fitted with $V_{0.5}$ = −33, q = 1.0 and n = 4 (see Fig. 4, legend). (*D*) The KAT1 currents recorded at pH_{in} = 6.2 and pH_{in} = 7.2 are scaled and compared. Each panel contains three sweeps; the KAT current recorded at pH_{in} = 7.2, the KAT1 current recorded at pH_{in} = 6.2, and the scaled KAT1 current recorded at pH_{in} = 6.2 with a 60-mV voltage shift. From left to right, the currents were recorded at −70, −90, and −110 mV at pH_{in} = 6.2 and at −130, −150, and −170 mV at pH_{in} = 7.2. Since the currents were first recorded at pH_{in} = 7.2 and then at pH_{in} = 6.2, any confounding by the rundown process, which shifts the voltage dependence to a more negative direction, would underestimate the low pH effects.

alone. Similarly, the hyperpolarization-activated currents recorded from the oocytes injected with both eag and KAT1 RNAs were not noticeably different from those recorded from the cells injected with KAT1 RNA alone. Similar results were obtained when KAT1 and *Shaker* with disrupted *N*-type inactivation (ShBΔ6-46 [Hoshi, Zagotta, and Aldrich, 1990]) RNAs were coinjected. KAT1 and IRK1 RNAs were also coinjected to see if they combined to form heteromultimeric channels. The currents recorded from the cells injected with both KAT1 and IRK1 RNAs did not noticeably differ from those expected from a simple summation of the wild-type KAT1 and IRK1 currents.

As with the KAT1 channel, the eag channel expressed in *Xenopus* oocytes also underwent the rundown process on patch excision as in the KAT1 channel. This eag channel rundown was not slowed down by internal ATP (1 mM). Unlike the rundown of the KAT1 channel, this eag channel rundown was not accompanied by a marked shift in the voltage dependence of activation. Furthermore, low pH_{in} = 6.2 did not induce the voltage shift as observed in the KAT1 channel.

DISCUSSION

Voltage-dependent Activation

Although the KAT1 channel is activated by hyperpolarization, the amino acid sequence analysis shows that its structural organization is more similar to that of the depolarization-activated *Shaker* K^+ channel with the S4 segment than to the cloned inward rectifier channels typified by ROMK1 (Ho, Vassilev, Kanazirska, Lytton, and Herbert, 1993), IRK1 (Kubo et al., 1993*a*) and GIRK1 (Kubo et al., 1993*b*). The preliminary characterization of the KAT1 macroscopic currents presented suggests that the underlying gating properties of the KAT1 channel are at least qualitatively similar to those of the *Shaker*-like depolarization-activated K^+ channels (e.g., Zagotta et al., 1994*b*). In the KAT1 channel, neither the open channel $i(V)$ characteristic nor the internal divalent block account for the overall voltage dependence of the channel, strongly indicating that the voltage-dependent gating of the KAT1 channel is intrinsic. About five to six equivalent charges or ~1.4 charges per subunit are involved in the activation process of the KAT1 channel. About 50% of the total charge movement is associated with the closing transitions near the open state. The sigmoidal characteristics of the KAT1 activation kinetics are also at least qualitatively similar to those of the *Shaker* channel (Zagotta et al., 1994*b*). These results suggest that it may be possible to use the kinetic model developed to describe the *Shaker* K^+ channel (Zagotta, Hoshi, and Aldrich, 1994*a*) to explain the KAT1 channel gating behavior with some quantitative modifications.

Gating Mechanisms Involved in the Rundown

Many ion channels are regulated by various cytoplasmic factors. Experimentally, this is often observed as marked differences in the channel behavior in the cell-attached configuration and the excised-configurations of the patch clamp method. The rundown, where the current amplitude decreases when the patch is excised, is an example of how ion channels are regulated. Many different channels have been shown to undergo this rundown process, including voltage-dependent Ca^{2+} channels

(for review, see Bean, 1992). Some K^+ channels also undergo the rundown process. The IRK1 channel expressed in *Xenopus* oocytes does not function well in the excised configurations (Kubo et al., 1993*a*). In many voltage-dependent channels that undergo the rundown process, the current amplitude decreases without obvious changes in the kinetics, indicating that the rundown process involves a decrease in the number of channels available to activate. In the KAT1 channel, the ramp $I(V)$ curves obtained after patch excision suggest that a large shift in the activation curve to a more negative direction is responsible for the decrease in the current amplitude. It is not likely that the KAT1 rundown is caused by a decrease in the number of the KAT1 channels available to open. Thus, it should be possible to elicit the KAT1 currents if large enough voltage pulses are applied. Availability of the KAT1 mutant channels with the voltage dependence shifted to a more positive direction should make it easier to investigate this phenomenon. Other marked differences in the channel behavior in the cell-attached configuration and that observed in the excised configurations have also been observed. For example, Marom, Goldstein, Kupper, and Levitan (1993) have shown that the inactivation properties of a Kv3 delayed rectifier channel is dependent on the recording configuration.

Cytoplasmic Factors Involved in the KAT1 Channel Rundown

Numerous attempts have been made to slow and reverse the rundown process. In many channels, intracellular solutions with a variety of agents, such as cAMP and ATP, have been found to at least slow the rundown process (for review, see Bean, 1992; Horn and Korn, 1992). Furthermore, in some experiments, addition of protein kinases has been shown to retard the rundown process (Bean, 1992). Although no single universal factor that prevents the rundown has been identified, the available results suggest that phosphorylation may be required for the function of some channels.

The KAT1 channel rundown is slowed and reversed by addition of ATP. Since the effect of ATP in enhancing the KAT1 channel activity often persists after washing with ATP-free solution, direct binding of ATP as a simple agonist is probably not involved. Furthermore, it is likely that hydrolysis of ATP is involved in the ATP's action in restoring the KAT1 channel activity because AMP-PNP, a nonhydrolyzable analogue of ATP, is much less effective in restoring the channel activity. However, the results with PKA, BAP, and CIP do not readily support the idea that phosphorylation mediated by cAMP-dependent protein kinase is involved in the KAT1 channel rundown.

Voltage-dependence Shifts Induced by ATP, cGMP, and pH

ATP, cGMP, and low pH all induce shifts in the voltage dependence of the KAT1 channel activation. Since they do not appear to affect the equivalent charge movement noticeably, it is unlikely that they affect the voltage-sensing elements directly. cGMP shifts the activation curve to a more negative direction whereas ATP shifts it to a more positive direction. Based on the results presented and the sequence similarity of the KAT1 channel to other channels, the following hypothesis of the KAT1 channel regulation is possible. Voltage dependence of the KAT1 channel is regulated by the interaction between the segments of the channel involved in

determining the rate constants at 0 mV and the intracellular carboxyl domain containing the putative cyclic nucleotide binding sites. ATP hydrolysis-dependent mechanisms and low intracellular pH facilitate this interaction and it shifts the voltage dependence to a more positive direction. When cGMP is bound to the carboxyl domain, this interaction is inhibited, shifting the voltage dependence to a more negative direction.

The KAT1 channel closely resembles the eag channel activated by depolarization in the amino acid sequence. Although both the KAT1 and eag channels rundown on patch excision, their electrophysiological properties are different. For example, the KAT1 channel rundown is slowed by ATP whereas that of the eag channel is not. The rundown of the KAT1 channel is accompanied by a large shift in the voltage dependence and it is also shifted by low pH. In the eag channel, the rundown does not involve a marked shift in the voltage dependence and low pH does not shift it, either. Thus, the same mechanisms may be involved in the voltage shift observed during the rundown and that induced by low internal pH in the KAT1 channel. The amino-acid sequence similarity between the KAT1 and eag channels may be used to investigate the structural domains involved in the channel modulation.

I thank R. Aldrich and E. Shibata for comments on the manuscript, J. A. Hughes for technical assistance, and H. D. Taylor for his enthusiasm.

This work was supported in part by the Carver Trust.

Original version received 15 July 1994 and accepted version received 28 September 1994.

REFERENCES

Anderson, J. A., S. S. Huprikar, L. V. Kochian, W. J. Lucas, and R. F. Gaber. 1992. Functional expression of a probable *Arabidopsis thaliana* potassium channel in *Saccharomyces cerevisiae*. *Proceedings of the National Academy of Sciences, USA.* 89:3736–3740.

Bean, B. 1992. Whole-cell recording of calcium channel currents. *Methods in Enzymology.* 207:181–193.

Brüggemann, A., L. Pardo, W. Stühmer, and O. Pongs. 1993. *Ether-á-go-go* encodes a voltage-gated channel permeable to K^+ and Ca^{2+} and modulated by cAMP. *Nature.* 365:445–448.

Burton, F. L., and O. F. Hutter. 1990. Sensitivity to flow of intrinsic gating in inwardly rectifying potassium channel from mammalian skeletal muscle. *Journal of Physiology.* 424:253–261.

Cohen, I. S., D. DiFrancesco, N. K. Mulrine, and P. Pennefather. 1989. Internal and external K^+ help gate the inward rectifier. *Biophysical Journal.* 55:197–202.

Guy, H. R., S. R. Durell, J. Warmke, R. Drysdale, and B. Ganetzky. 1991. Similarities in amino acid sequences of *Drosophila* eag and cyclic nucleotide-gated channels. *Science.* 254:730.

Ho, K., P. M. Vassilev, M. V. Kanazirska, J. Lytton, and S. C. Hebert. 1993. The primary structure of a mammalian ATP-sensitive potassium channel and functional expression from complementary DNA. *Nature.* 362:31–38.

Horn, R., and S. J. Korn. 1992. Prevention of rundown in electrophysiological recording. *Methods in Enzymology.* 207:149–155.

Hoshi, T., W. N. Zagotta, and R. W. Aldrich. 1990. Biophysical and molecular mechanisms of *Shaker* potassium channel inactivation. *Science.* 250:533–538.

Hoshi, T., W. N. Zagotta, and R. W. Aldrich. 1994. *Shaker* potassium channel gating I: transitions near the open state. *Journal of General Physiology.* 103:249–278.

Kramer, R. H. 1990. Patch cramming: monitoring intracellular messengers in intact cells with membrane patches containing detector ion channels. *Neuron.* 4:335–341.

Kubo, Y., T. J. Baldwin, Y. N. Jan, and L. Y. Jan. 1993*a*. Primary structure and functional expression of a mouse inward rectifier potassium channel. *Nature.* 362:127–132.

Kubo, Y., E. Reuveny, P. A. Slesinger, Y. N. Jan, and L. Y. Jan. 1993*b*. Primary structure and functional expression of a rat G-protein–coupled muscarinic potassium channel. *Nature.* 364:802–806.

MacKinnon, R. 1991. Determination of the subunit stoichiometry of a voltage-activated potassium channel. *Nature.* 350:232–235.

Marom, S., S. A. N. Goldstein, J. Kupper, and I. B. Levitan. 1993. Mechanism and modulation of inactivation of the Kv3 potassium channel. *Receptors and Channels.* 1:81–88.

Matsuda, H. 1991. Magnesium gating of the inwardly rectifying K+ channel. *Annual Review of Physiology.* 53:289–298.

Pennefather, P., C. Oliva, and N. Mulrine. 1992. Origin of the potassium and voltage dependence of the cardiac inwardly rectifying K-current (IK1). *Biophysical Journal.* 61:448–462.

Ruppersberg, J. P., K. H. Schroter, B. Sakmann, M. Stocker, S. Sewing, and O. Pongs. 1990. Heteromultimeric channels formed by rat brain potassium-channel proteins [see comments]. *Nature.* 345:535–537.

Salkoff, L., K. Baker, A. Butler, M. Covarrubias, M. D. Pak, and A. Wei. 1992. An essential 'set' of K+ channels conserved in flies, mice and humans. *Trends in Neuroscience.* 15:161–166.

Schachtman, D. P., J. I. Schroeder, W. J. Lucas, J. A. Anderson, and R. F. Gaber. 1992. Expression of an inward-rectifying potassium channel by the Arabidopsis KAT1 cDNA. *Science.* 258:1654–1658.

Schoppa, N. E., K. McCormack, M. A. Tanouye, and F. J. Sigworth. 1992. The size of gating charge in wild-type and mutant *Shaker* potassium channels. *Science.* 255:1712–1715.

Schroeder, J. 1988. K^+ transport properties of K^+ channels in the plasma membrane of *Vicia faba* guard cells. *Journal of General Physiology.* 92:667–683.

Schroeder, J. I., R. Hedrich, and J. M. Ferandez. 1984. Potassium-selective single channels in guard cell protoplasts of *Vicia faba. Nature.* 312:361–362.

Schroeder, J. I., K. Raschke, and E. Neher. 1987. Voltage-dependent K^+ channels in guard cell protoplasts. *Proceedings of the National Academy of Sciences, USA.* 84:4108–4112.

Sentenac, H., N. Bonneaud, M. Minet, F. Lacroute, J. M. Salmon, F. Gaymard, and C. Grignon. 1992. Cloning and expression in yeast of a plant potassium ion transport system. *Science.* 256:663–665.

Silver, M. R., and T. E. DeCoursey. 1990. Intrinsic gating of inward rectifier in bovine pulmonary artery endothelial cells in the presence or absence of internal Mg^{2+}. *Journal of Physiology.* 425:145–167.

Warmke, J., R. Drysdale, and B. Ganetzky. 1991. A distinct potassium channel polypeptide encoded by the *Drosophila* eag locus. *Science.* 252:1560–1562.

Zagotta, W. N., T. Hoshi, and R. W. Aldrich. 1989. Gating of single *Shaker* potassium channels in *Drosophila* muscle and in *Xenopus* oocytes injected with *Shaker* mRNA. *Proceedings of the National Academy of Sciences, USA.* 86:7243–7247.

Zagotta, W. N., T. Hoshi, and R. W. Aldrich. 1990. Restoration of inactivation in mutants of *Shaker* potassium channels by a peptide derived from ShB. *Science.* 250:568–571.

Zagotta, W. N., T. Hoshi, and R. W. Aldrich. 1994*a*. *Shaker* potassium channel gating III. Evaluation of kinetic models for activation. *Journal of General Physiology.* 103:321–362.

Zagotta, W. N., T. Hoshi, J. Dittman, and R. W. Aldrich. 1994*b*. *Shaker* potassium channel gating II. Transitions in the activation pathway. *Journal of General Physiology.* 103:279–319.